



High-pressure structural phase transitions and electronic properties of the alkali hydride compounds XH (X=K, Rb and Cs)



Raed Jaradat ^a, Mohammed Abu-Jafar ^{a,*}, Issam Abdelraziq ^a, Saad Bin Omran ^b, Diana Dahliah ^a, Rabah Khenata ^c

^a Physics Department, An Najah National University, Nablus, Palestine

^b Department of Physics and Astronomy, College of Science, King Saud University, P.O.Box 2455, Riyadh 11451, Saudi Arabia

^c Laboratoire de Physique Quantique de la Matière et de la Modélisation, Mathématique (LPQ3M), Université de Mascara, Mascara, 29000, Algeria

HIGHLIGHTS

- mBJ-GGA and YS-PBE0 convert the CsCl structure from semiconductor to insulator for KH and RbH.
- mBJ-GGA and YS-PBE0 convert the CsCl structure from semiconductor to wide energy-band gap semiconductor for CsH.
- Three phase transitions have been predicted in this work, from RS to CsCl, RS to ZB and RS to WZ, for each compound.
- Under low pressure, the RS structure expands and transforms into WZ and ZB only when V/V_0 is greater than one.

ARTICLE INFO

Article history:

Keywords:
Phase transitions
Alkali hydride
FP-LAPW
mBJ potential

ABSTRACT

The equilibrium structural parameters, structural phase transition as well the electronic properties of XH compounds have been computed by using the first-principles calculations based on density-functional theory (DFT) and the full-potential linearized augmented plane-wave (FP-LAPW) method. The generalized gradient approximation (GGA) has been used for the exchange-correlation potential. The equilibrium structural parameters such as the lattice constant, the bulk modulus and the pressure-induced phase transition were calculated for rocksalt (RS), cesium chloride (CsCl), zincblende (ZB) and wurtzite (WZ) structures. The GGA, modified Becke-Johnson (mBJ-GGA) and Yukawa screened hybrid functional (YS-PBE0) schemes have been used to calculate the electronic properties. The mBJ-GGA and YS-PBE0 schemes have been found to be more accurate than GGA in computing the energy-band gap. An agreement of our results with the experimental and results of the other theoretical work indicate its reliability. The compounds under our investigation are found to be wide band gap semiconductors within the GGA, and insulators using the mBJ-GGA and YS-PBE0 approaches.

© 2018 Elsevier B.V. All rights reserved.

1. Introduction

Hydrogen is the lightest element in the periodic table, that is why alkali hydrides XH (X = Li, Na, K, Rb and Cs) have the simplest structures. These compounds have diverse technological applications such as hydrogen storage and high-energy fuels [1]. Generally, these types of compounds are, soft solids: their bulk moduli gradually decrease from Li to Cs, while their lattice constant increases. From the previous experimental work it has been reported that these types of compounds crystallize in the rocksalt structure

at atmospheric pressure and room temperature. The structural phase transition of NaH, KH, RbH and CsH compounds from the low-pressure rocksalt (B1) structure to the high-pressure cesium chloride (B2) structure has been observed in diamond-anvil-cell high-pressure experiments, while the B1 to B2 phase transition in LiH has not yet been observed [2–4]. The transition pressures for these compounds decreases as the alkali atomic mass increases. NaH has a huge transition pressure compared to the others, which is approximately 30 GPa, and a volume fraction $V/V_0 = 0.61 \pm 0.01$ [3]. The KH, RbH and CsH transition pressures are 4.0, 2.2 and 1.2 GPa, respectively [4]. The transition pressures of CsH, RbH, and KH are found to be 28 GPa measured by performing the high-pressure energy-dispersive X-ray studies [4], which is in excellent

* Corresponding author.

E-mail address: mabujafar@najah.edu (M. Abu-Jafar).

agreement with the result obtained from the equation of state. However the calculation of transition pressure of NaH is excluded in their experiment. Sudha et al. [5] used the Vienna package to investigate the structural, electronic, elastic and their related properties of the alkali hydrides XH ($X = \text{Li}, \text{Na}, \text{K}, \text{Rb}, \text{Cs}$) in the rocksalt and cesium chloride structures; these compounds were reported to be semiconductors with the CsCl structure. The B1 to B2 transition pressures were predicted to be 208.0, 37.0, 3.5, 3.0 and 2.1 GPa for LiH, NaH, KH, RbH and CsH, respectively, using the GGA approach [5]. Xiao-Wei et al. [6] used an ab initio plane-wave pseudo-potential density-functional theory method to investigate the phase transition from the B1 to B2 structures and the bulk modulus of NaH; the transition pressure was predicted to be 32 GPa, and the bulk modulus was found to decrease as the temperature increases. Saitta et al. [7] carried out DFT calculations within the local-density approximation (LDA) and its gradient-corrected (GC) generalization using pseudo-potentials to calculate the transition pressure for CsH from the B1 to B2; pressures of –0.8 and 1.5 GPa were obtained using the LDA and GC approaches, respectively. Rodriguez et al. [8] applied an improved linear muffin-tin orbital atomic-sphere approximation-energy approach to investigate the static structural properties and the pressure-induced phase transition from B1 to B2 for the NaH and KH compounds; the estimated transition pressures were found to be 30.7 and 2.0 GPa for NaH and KH, respectively. Ahuja et al. [9] used the full-potential linear-muffin-tin-orbital (FP-LMTO) method to theoretically investigate the LiH, NaH, KH and RbH compounds. These authors predict that RbH and KH will transform to CsCl structure, while their calculations predict CrB crystal structures at high pressure for RbH and KH but not for the light alkali compounds, NaH and LiH. Jaradat et al. [10] used the full-potential linearized augmented plane wave (FP-LAPW) method implemented in Wien2k package to investigate the structural, electronic properties and the pressure-induced phase transition of alkali hydrides XH ($X = \text{Li}, \text{Na}$) in the rocksalt, cesium chloride, zinc-blende and wurtzite structures; these compounds were predicted to be semiconductors with the CsCl structure and the pressure-induced phase transition from the RS to CsCl were found to be 211.8 and 34.26 GPa for LiH and NaH, respectively, while from the RS to ZB were found to be –3.83 and –1.94 GPa for LiH and NaH, respectively and from RS to WZ were –2.4 and –1.57 GPa for LiH and NaH, respectively.

From the above discussions, we can see that the researchers have studied these compounds in the rocksalt and cesium chloride structures, but there are no previous reports on these types of compounds in the zincblende (ZB) and wurtzite (WZ) phases. The structural, electronic properties as well as the structural phase transitions of the alkali hydrides XH ($X = \text{K}, \text{Rb}$ and Cs) are investigated in this work in the RS, CsCl, ZB and WZ structures using the full-potential linearized augmented plane-wave method (FP-LAPW) in order to complement existing theoretical works on alkali hydride compounds.

2. Methods of calculations

The first-principles calculations of the alkali hydrides are performed in four different structures (RS, CsCl, ZB and WZ) using the (FP-LAPW) method [11] based on the density-functional theory (DFT) [12] and implemented in WIEN2k code [13]. Generalized gradient approximation (GGA-PBE) [14] has been used to predict the pressure-induced structural transitions from RS to the other structures and to calculate the structural properties. The modified Becke-Johnson (GGA-mBJ) [15,16] and Yukawa screened hybrid functional (YS-PBEO) [17] approaches have also been used to

overcome the severe underestimation of the excited-state properties using GGA approach, such as the band-gap values for many semiconductors and insulators.

To study the region near the nucleus without introducing pseudo potential, the basis set must be efficient. Therefore, the atomic space is divided into the following two regions: the muffin-tin region and the interstitial region. The muffin-tin region is the space occupied by spheres of radius R_{MT} , one around each atom; these spheres are often called muffin-tin (MT) spheres. The remaining space outside the spheres is called the interstitial region. The product of the spherical-harmonic expansion and the radial function, along with their first derivatives, are linearized to form the basis functions used inside the MT spheres, and plane-wave basis set is used in the interstitial part of the unit cell. The muffin tin radii (R_{MT}) used in the present calculations for the H, K, Rb and Cs atoms are 1.4a.u., 2.6a.u., 2.67a.u and 2.76a.u., respectively. The charge density was Fourier expanded up to $G_{\max} = 20$ in RS, CsCl and ZB, and up to $G_{\max} = 14$ in the WZ structure. The plane-wave cutoff was chosen such that $R_{\text{MT}}K_{\max} = 5$.

The basis functions, charge density and potential are expanded inside the muffin-tin spheres in combination with the spherical harmonic functions, with a cut-off $l_{\max} = 12$ for the WZ structure and $l_{\max} = 6$ for the cubic structures. For energy convergence, the full Brillouin zones (FBZ) were sampled at 1331 k-points for the three cubic structures, RS, CsCl and ZB, with a grid size of $11 \times 11 \times 11$, which is reduced to 56 special k-points in the irreducible Brillouin zones (IBZ); and 3700 k-points for the WZ structure with a grid size of $18 \times 18 \times 10$, which is reduced to 222 special k-points in the IBZ [18]. The iteration process was repeated until the calculated total energy of the crystal converged to less than 10^{-5} Ry/unit cell.

3. Results and discussions

3.1. Structural properties

The ground-state properties of alkali hydrides for each structure have been estimated by calculating the total energy at different unit-cell volumes and fitting the calculated energy versus volume (E-V) curves to Murnaghan's equation of state (EOS) [19], as shown in Figs. 1–3 for the KH, RbH and CsH compounds, respectively, with RS, CsCl, ZB and WZ structures. It is clearly seen from these curves that the rocksalt structure has the lowest energy minimum at ambient pressure, which means that it is the most stable structure at normal conditions.

The calculated equilibrium lattice constant a_0 , bulk modulus B_0 and first-order pressure derivatives of the bulk modulus B'_0 for KH, RbH and CsH in the RS, CsCl, ZB and WZ phases, along with the available experimental [2,4,20–22] and theoretical [5,23–26] results are listed in Tables 1–3. It is clear that the lattice constants for all phases increase as the X radii increase, while the bulk moduli decrease. Table 1 shows that the calculated structural parameters for KH, RbH and CsH in RS structure are in good agreement with the experimental results. From Table 2, it is clear that the calculated structural parameters for KH, RbH and CsH in the CsCl structure are in good agreement with the results of Sudha et al. [5].

The calculated structural parameters for KH, RbH and CsH in the ZB structure are presented in Table 3: the lattice constant increases as the alkali radius increases, while the bulk modulus decreases. Table 4 displays the structural parameters for the alkali compounds in the WZ structure. We can see that the lattice constant and c/a ratio increase as the alkali radius increases; the c/a ratios are approximately 1.5142, 1.5265 and 1.5480 for KH, RbH and CsH, respectively.

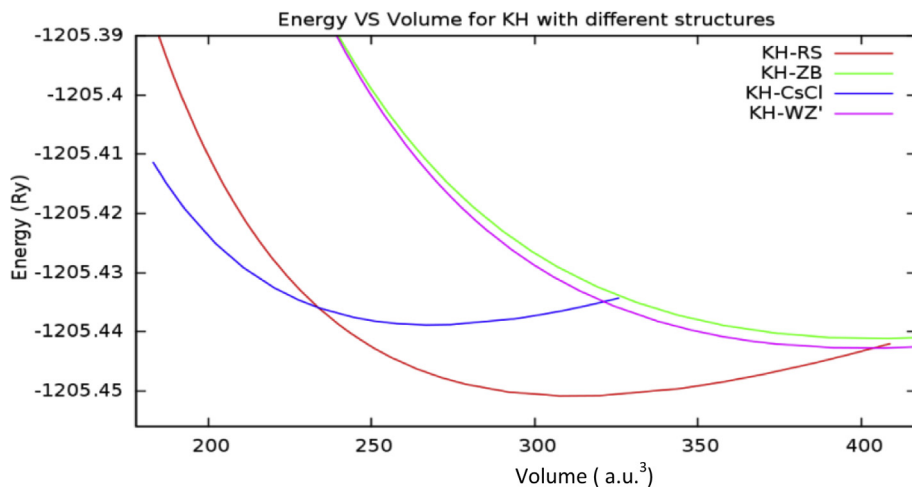


Fig. 1. Calculated total energy per unit cell versus cell volume for KH in RS, CsCl, ZB and WZ structures.

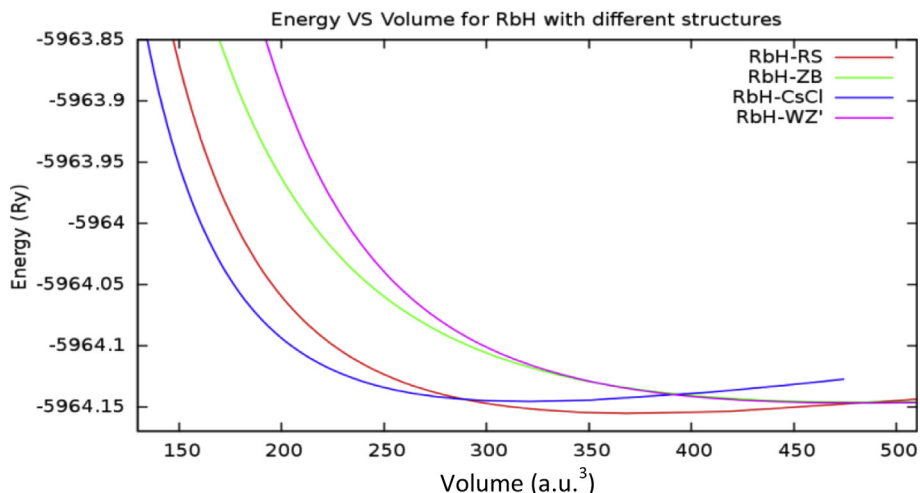


Fig. 2. Calculated total energy per unit cell versus cell volume for RbH in RS, CsCl, ZB and WZ structures.

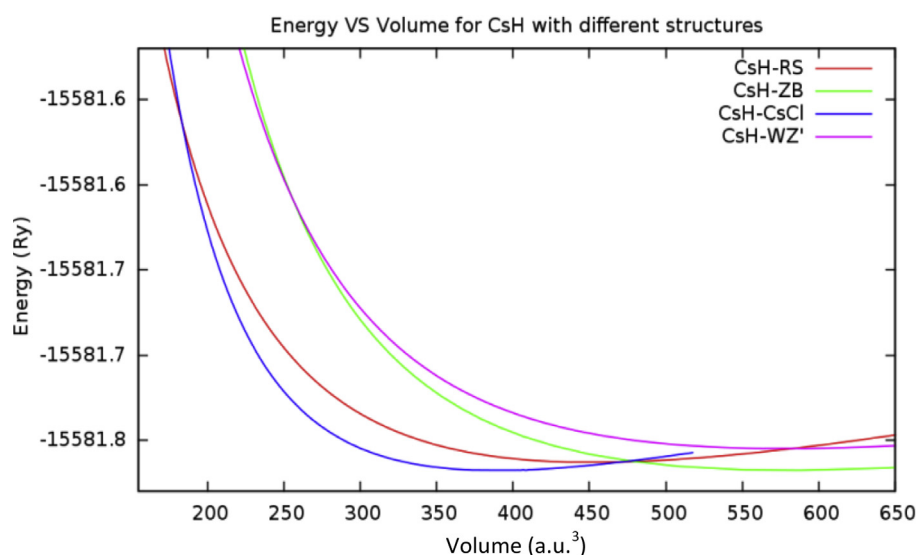


Fig. 3. Calculated total energy per unit cell versus cell volume for CsH in RS, CsCl, ZB and WZ structures.

Table 1

Structural parameters for KH, RbH and CsH in RS structure, along with experimental and other theoretical results.

Compound	Structural parameters	Present work	Experimental work	Other theoretical work
KH	$a_0(\text{\AA})$	5.70	5.70 ^{d, e}	5.721 ^c , 5.701 ⁱ
	$B_0(\text{GPa})$	13.41	15.6 \pm 1.5 ^b	16 ^c , 17.3 ^g
	B'	3.9	4.0 \pm 0.5 ^b	2.95 ^c
RbH	$a_0(\text{\AA})$	6.054	6.037 ^e , 6.048 ^d	5.992 ^c , 6.199 ⁱ , 6.064 ^f
	$B_0(\text{GPa})$	11.25	10.0 \pm 1.0 ^b	14.1 ^c , 14.7 ^g
	B'	3.87	3.9 \pm 0.5 ^b	2.840 ^c
CsH	$a_0(\text{\AA})$	6.446	6.376 ^e , 6.387 ^{a, e}	6.344 ^c , 6.407 ⁱ
	$B_0(\text{GPa})$	8.9	8.0 \pm 0.7 ^a , 7.6 \pm 0.8 ^b	12 ^c , 11.9 ^g , 8.8 ^h
	B'	3.26	4.0 ^a , 4 \pm 0.4 ^b , 4.0 ^d	3.037 ^c

^aRef. [2].^bRef [4].^cRef [5].^dRef [20].^eRef [21].^fRef [23].^gRef [24].^hRef [25].ⁱRef [26].**Table 2**

Structural parameters for KH, RbH and CsH in CsCl structure, along with experimental and other theoretical results.

Compound	Structural parameters	Present work	Experimental work	Other theoretical work
KH	$a_0(\text{\AA})$	3.41		3.520 ^c
	$B_0(\text{GPa})$	15.04	28.5 \pm 1.5 ^b	20 ^c
	B'	4.00	4.0 + 0.6 ^b	3.007 ^c
RbH	$a_0(\text{\AA})$	3.62		3.81 ^c
	$B_0(\text{GPa})$	13.64	18.4 \pm 1.1 ^b	14.9 ^c
	B'	4.21	3.9 + 0.5 ^b	2.866 ^c
CsH	$a_0(\text{\AA})$	3.863		3.84 ^c
	$B_0(\text{GPa})$	11.50	14.2 \pm 1 ^a , 22.3 \pm 1.5 ^b , 15.9 ^d	14 ^c
	B'	4.45	4 \pm 0.2 ^a , 4.8 \pm 0.5 ^b	4.675 ^c

^aRef. [2].^bRef [4].^cRef [5].^dRef [22].**Table 3**

Structural parameters for KH, RbH and CsH in ZB structure.

Compound	$a_0(\text{\AA})$	$B_0(\text{GPa})$	B'
KH	6.215	9.85	3.40
RbH	6.598	8.33	3.25
CsH	7.002	6.47	3.57

Table 4

Structural parameters for KH, RbH and CsH in WZ structure.

Compound	$a_0(\text{\AA})$	c/a	$u(\text{a.u.})$	$B(\text{GPa})$	B'
KH	4.492	1.514	0.393	10.12	3.62
RbH	4.764	1.527	0.390	8.135	4.06
CsH	5.037	1.548	0.389	6.374	3.71

3.2. Phase transition

The energy per unit cell is calculated by using the GGA at different unit-cell volumes, and the results are fitted to the Murnaghan equation of state, as shown in Figs. 1–3. It is clearly shown that these compounds undergo a structural phase transition from RS to the other structures. To determine the pressure-induced structural phase transition, the Gibbs free energy (G) for each phase must be calculated, which is given by $G = H - TS$ or $G = E_0 + PV$.

TS. The calculations are carried out at $T = 0$ K, which leads to equality between the Gibbs free energy and the enthalpy, $H = E_0 + PV$. At the transition pressure, the enthalpies of the two consecutive phases are equal. Enthalpy-pressure curves for KH, RbH and CsH are displayed in Figs. 4–6.

The estimated induced-transition pressures from RS to the other structures for KH, RbH and CsH compounds are presented in Table 6. The computed transition pressures from RS to CsCl structures are found to be equal to 5.11, 3.5 and 2.45 GPa, which are in good agreement with the experimental values of 4.0, 2.2 and 1.2 GPa for KH, RbH and CsH, respectively [4]. Table 5 displays the V/V_0 fraction, where V is the unit-cell volume at which the transition occurs and V_0 is the unit-cell equilibrium volume of the RS structure. The induced-transition pressures from RS to CsCl for KH, RbH and CsH occurred at $V/V_0 = 0.693$, 0.719 and 0.736, which means that the RS to CsCl transition requires volume compression. It is clear that the V/V_0 fraction increases as the alkali radius increases, which means that a lower induced-transition pressure is needed. The RS to ZB and RS to WZ phase transitions occur when V/V_0 is greater than one, meaning that these two transitions require volume expansion. Table 6 shows that the RS to WZ transition pressure increases from KH to CsH, while the RS to ZB transition pressure decreases.

There are small differences between the reported and experimental transition pressures, and one of the reasons for this

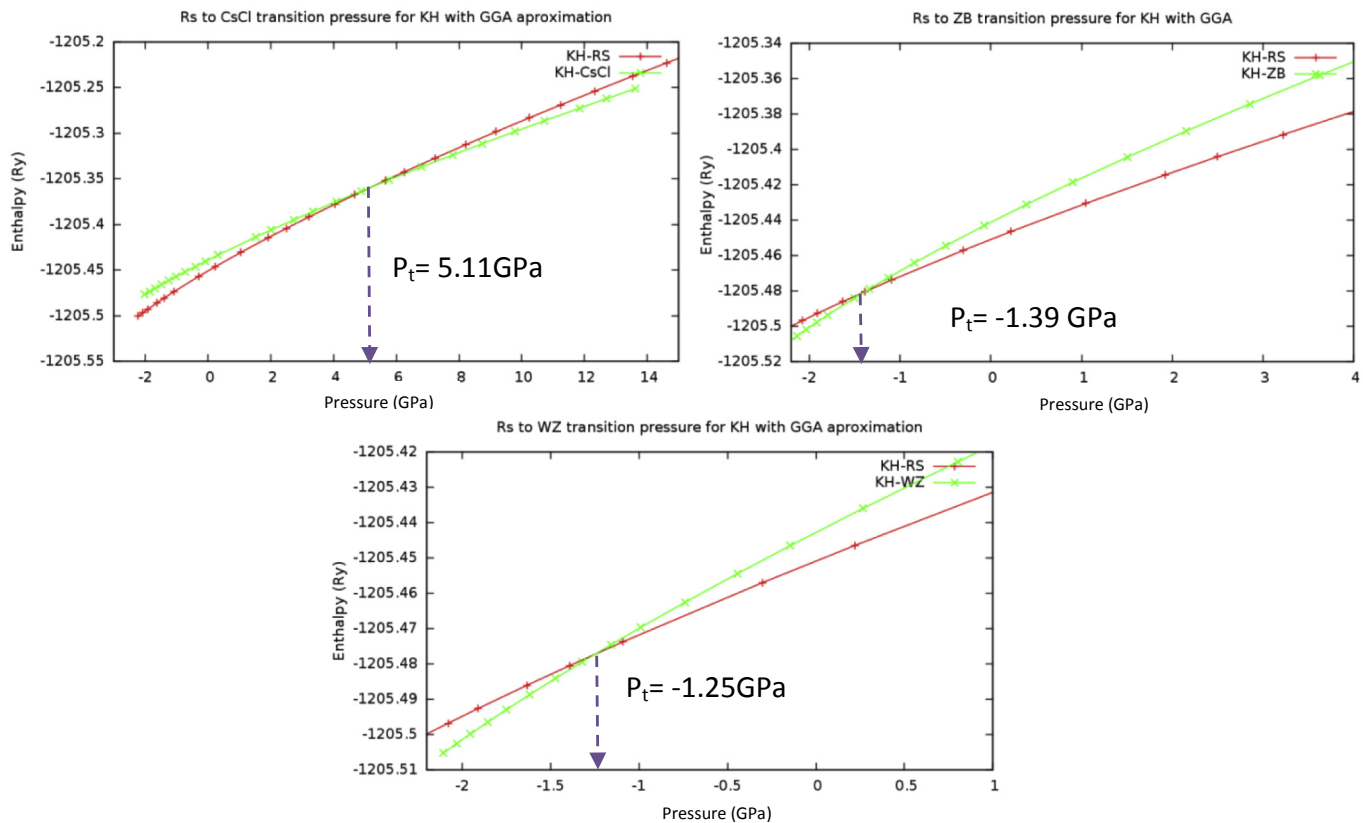


Fig. 4. Enthalpy as a function of pressure for KH using the GGA method.

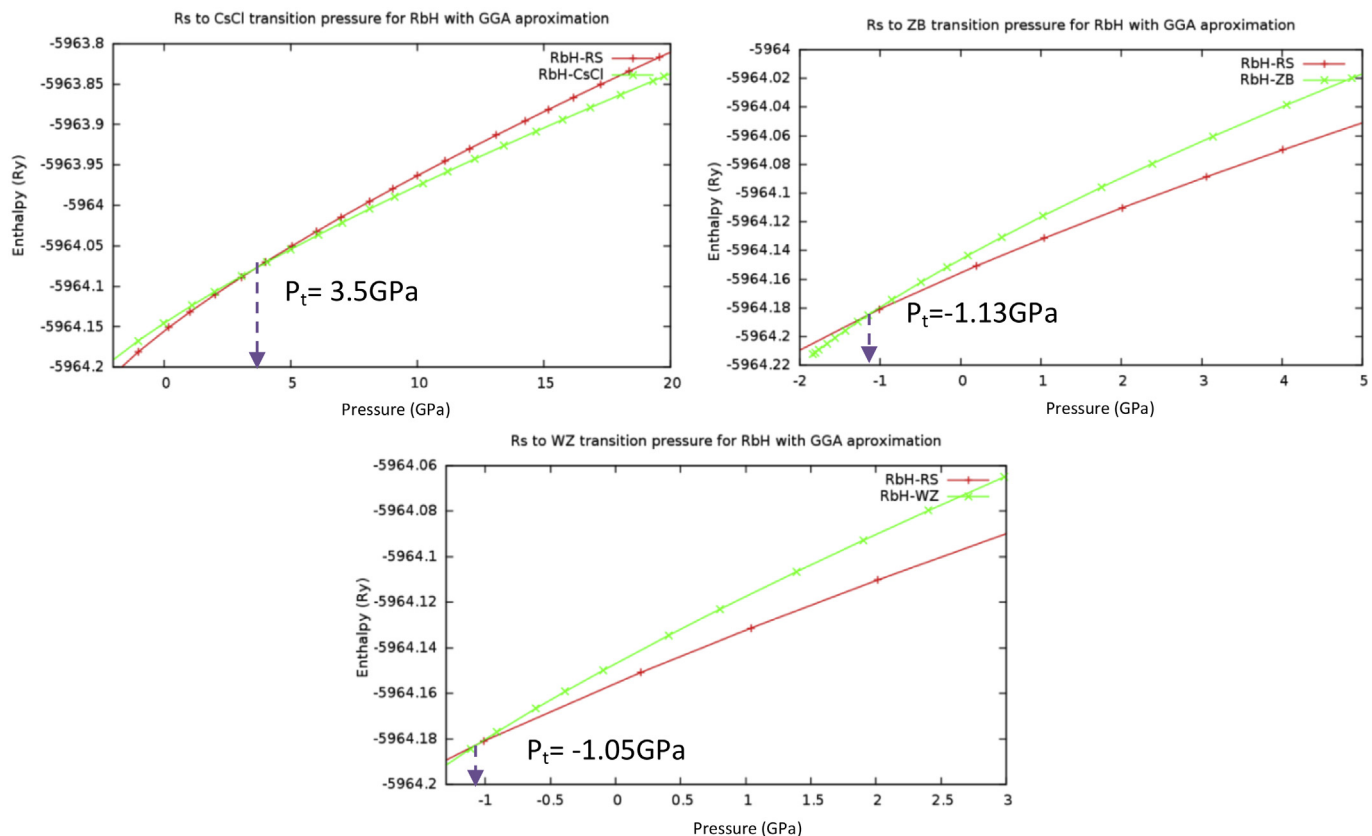


Fig. 5. Enthalpy as a function of pressure for RbH using the GGA method.

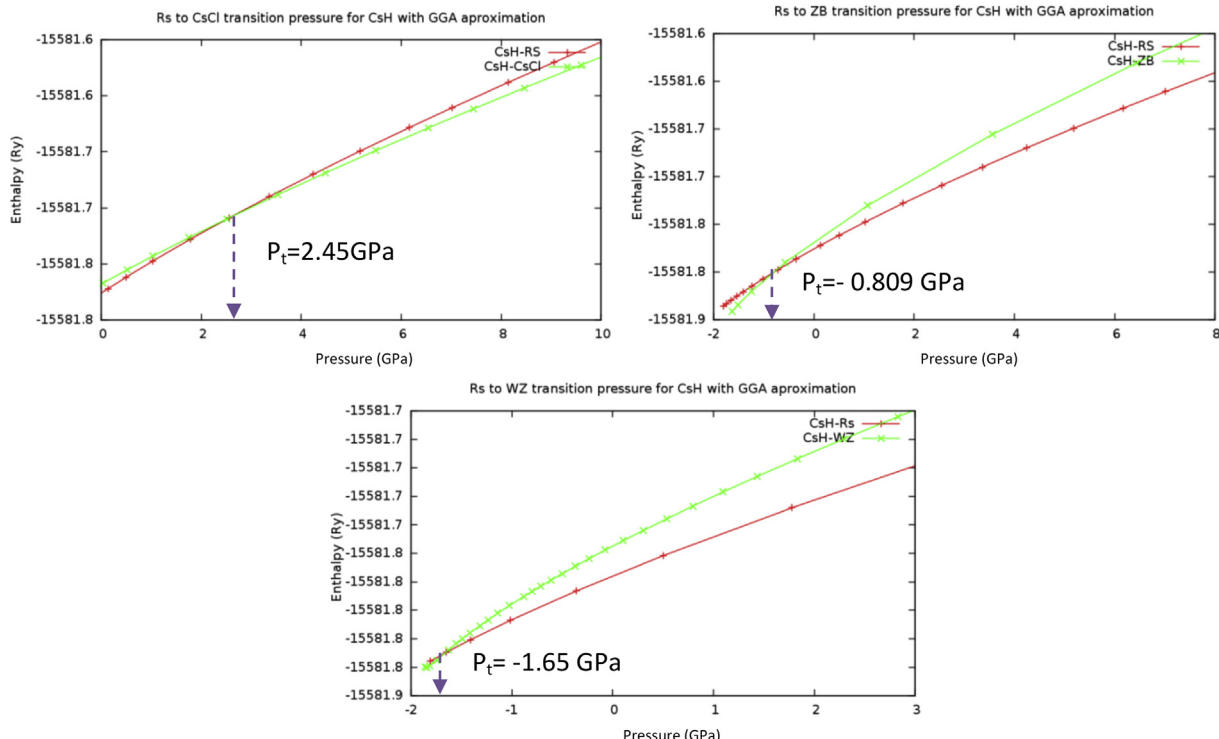


Fig. 6. Enthalpy as a function of pressure for CsH using the GGA method.

Table 5

The V/V_0 fractions for KH, RbH and CsH.

Compound	RS → CsCl	RS → ZB	RS → WZ
V/V_0 for KH	0.693	1.571	1.513
V/V_0 for RbH	0.719	1.546	1.554
V/V_0 for CsH	0.736	1.511	2.373

discrepancy is that the experimental calculations are carried out at room temperature, while the theoretical calculations are performed at 0K, the induced transition pressure decreases as the temperature increases. Table 6 reports the computed transition pressures for the KH, RbH and CsH compounds along with the previous theoretical [5,7–9] and experimental results [4].

3.3. Electronic properties

Atoms in a crystal interact with their neighbors and the energy levels of the electrons in isolated atoms turn into bands. As a matter of fact, a material can be classified as a conductor, insulator or semiconductor by examining its band structure and the Fermi

energy-level position. The self-consistent band structures of KH, RbH and CsH are calculated at equilibrium lattice constants in RS, CsCl, ZB and WZ structures by using the GGA, mBJ-GGA and YSPBE0 approximations for the exchange-correlation potential. The results are shown in Figs. 7–9. We can see clearly that the Fermi level crosses the energy-band gap for all structures. The topologies of the energy-band structures for KH, RbH and CsH compounds are quite similar to one another. The minimum energy-band gap is direct along the L-point and the X-point symmetry lines within the RS and ZB structures for RbH and CsH compounds, respectively, while it is direct along the L-point and the M-point symmetry lines within RS and WZ, respectively for KH compound with GGA, mBJ-GGA and YSPBE0 approaches. For the CsCl structure, the minimum energy-band gap is indirect for all compounds, except for CsH with mBJ-GGA, where it is direct along the R-point symmetry line. RbH compound has a direct minimum energy-band gap along the M-point symmetry line within the WZ structure with GGA and YSPBE0, but it is indirect with mBJ-GGA. CsH compound has a direct minimum energy-band gap along the M-point symmetry line within the WZ structure with mBJ-GGA, but it is indirect with GGA and YSPBE0. From Figs. 7–9, it is clear that the electronic energy

Table 6

Calculated transition pressures as well as the experimental and other theoretical data for KH, RbH and CsH.

Compound	RS → CsCl P_t (GPa)			RS → ZB P_t (GPa)	RS → WZ P_t (GPa)
	Present Work	Experimental work	Other theoretical work		
KH	5.11	4 ^a	3.5 ^{b, e} , 2 ^d	-1.39	-1.25
RbH	3.50	2.2 → 3.1 ^a	3 ^b , 1 ^e	-1.13	-1.05
CsH	2.45	1.2 ^a	2.1 ^b , 1.5 ^c	-0.81	-1.65

^aRef. [4].

^bRef [5].

^cRef [7].

^dRef [8].

^eRef [9].

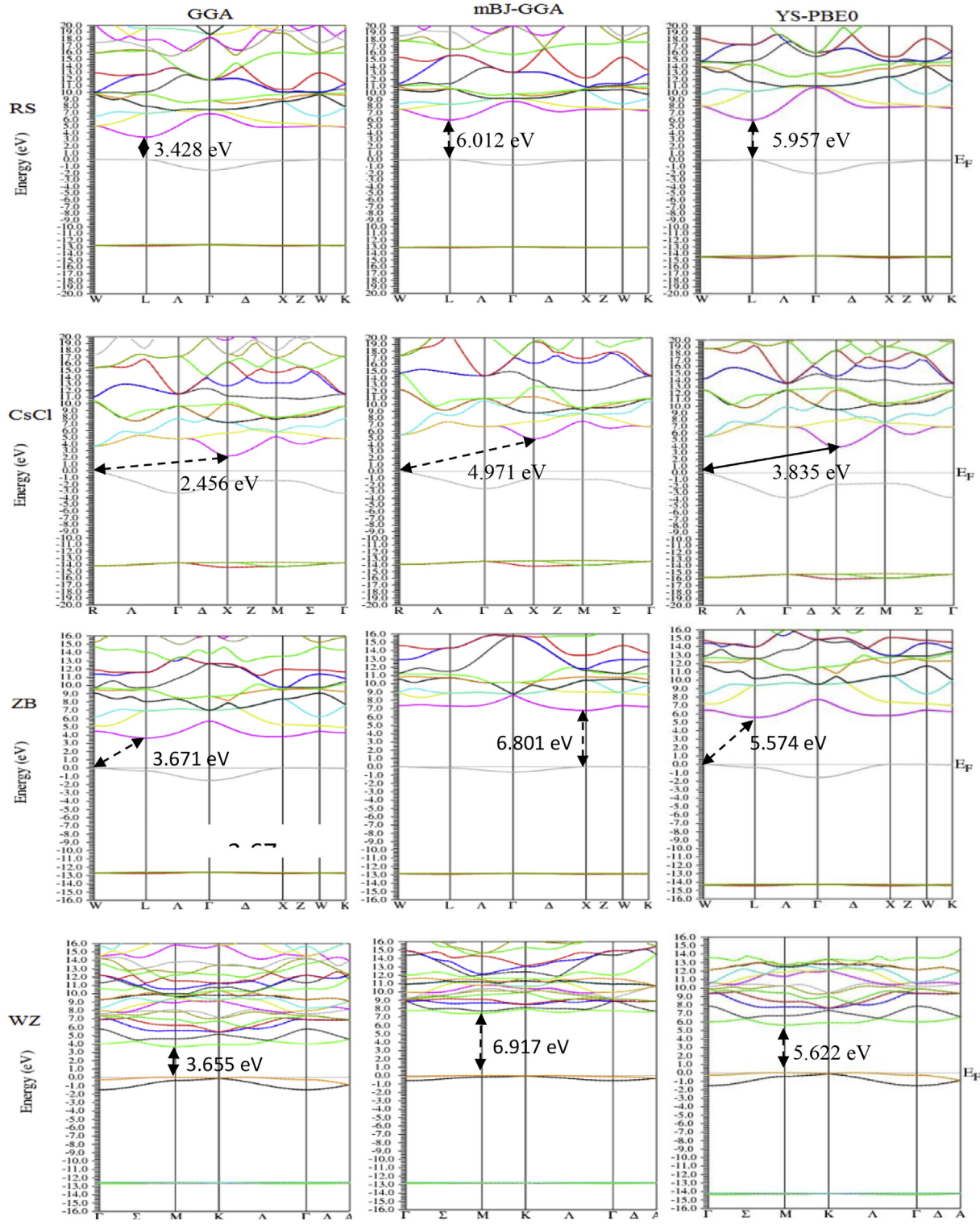


Fig. 7. Band structure of KH in RS, CsCl, ZB and WZ using the GGA, mBJ-GGA and YS-PBE0 approaches.

bands are more vertically distributed with GGA; mBJ-GGA and YS-PBE0 shift them closer to one another.

Differences in the width of the first valence band below the Fermi-energy between GGA and mBJ-GGA within RS, CsCl, ZB and WZ are 0.6, 1.1, 0.9 and 0.9 eV, respectively, for KH; 0.8, 0.82, 0.81

and 0.80 eV, respectively for RbH; and 0.60, 0.58, 0.64 and 0.60 eV, respectively for CsH, while the difference between GGA and YS-PBE0 are 0.4, 0.43, 0.4 and 0.0 eV, respectively for KH and 0.0, 0.22, 0.0 and 0.0 eV, respectively for RbH and 0.22, 0.1, 0.07 and 0.0, respectively for CsH. Table 7 reports the energy-band gaps,

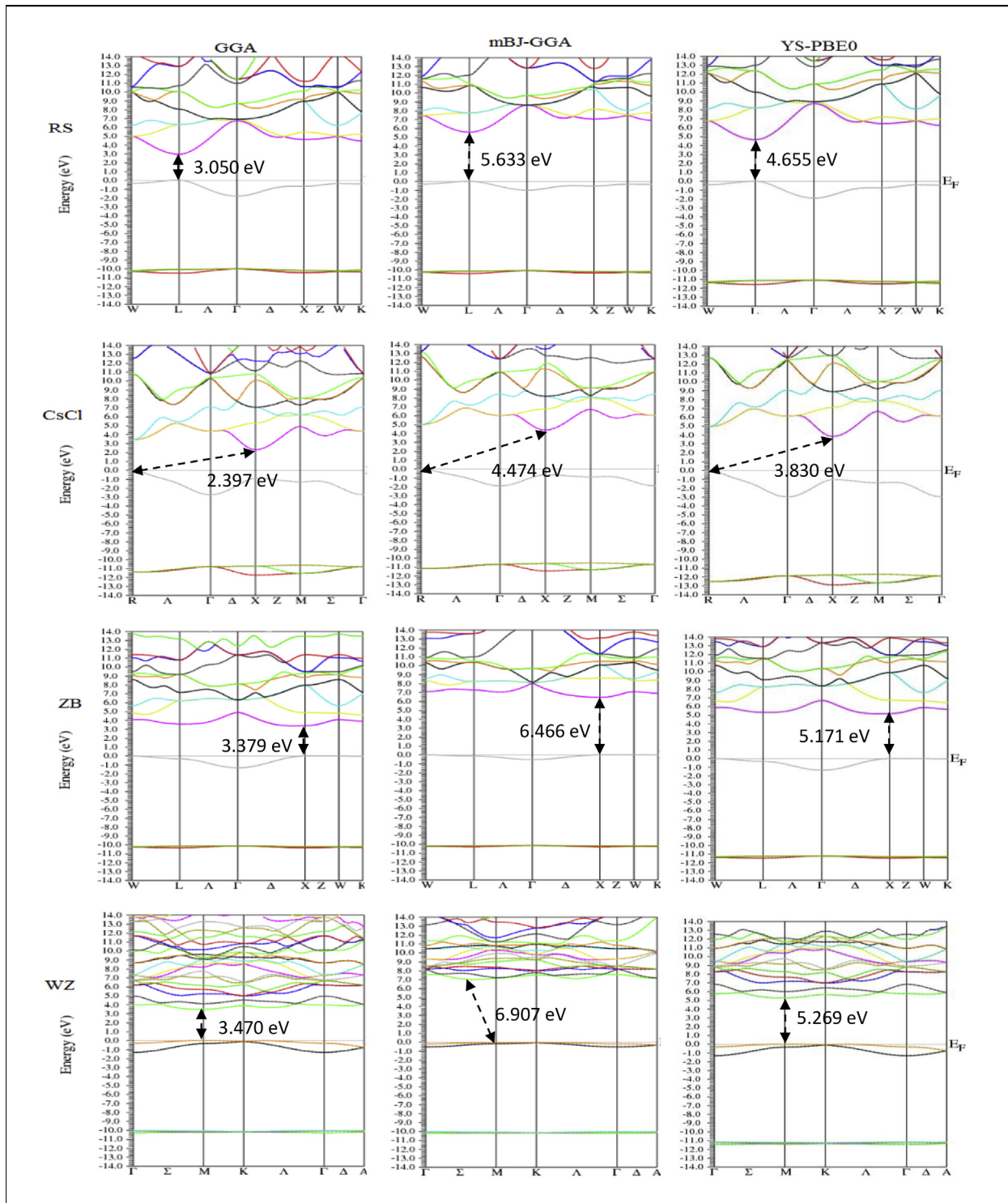


Fig. 8. Band structure of RbH in RS, CsCl, ZB and WZ using the GGA, mBJ-GGA YS-PBE0 approaches.

calculated using the three approaches, YS-PBE0, mBJ-GGA and GGA along with the available theoretical [5,27–32] and experimental [33,34] results.

The calculated energy-band gaps are broader using YS-PBE0 and mBJ-GGA than using GGA, by approximately 0.59 eV–2.53 eV using YS-PBE0 and 1.25 eV to 3.4 eV using mBJ-GGA, depending on which

structure is used; they vary from one compound to another. The energy-band gap has been modified using the mBJ-GGA and YS-PBE0 approaches, so the band gap calculated using mBJ-GGA and YS-PBE0 are more accurate than that calculated using the GGA approach and they are in good agreement with experimental results. The present calculations using mBJ-GGA are greater than

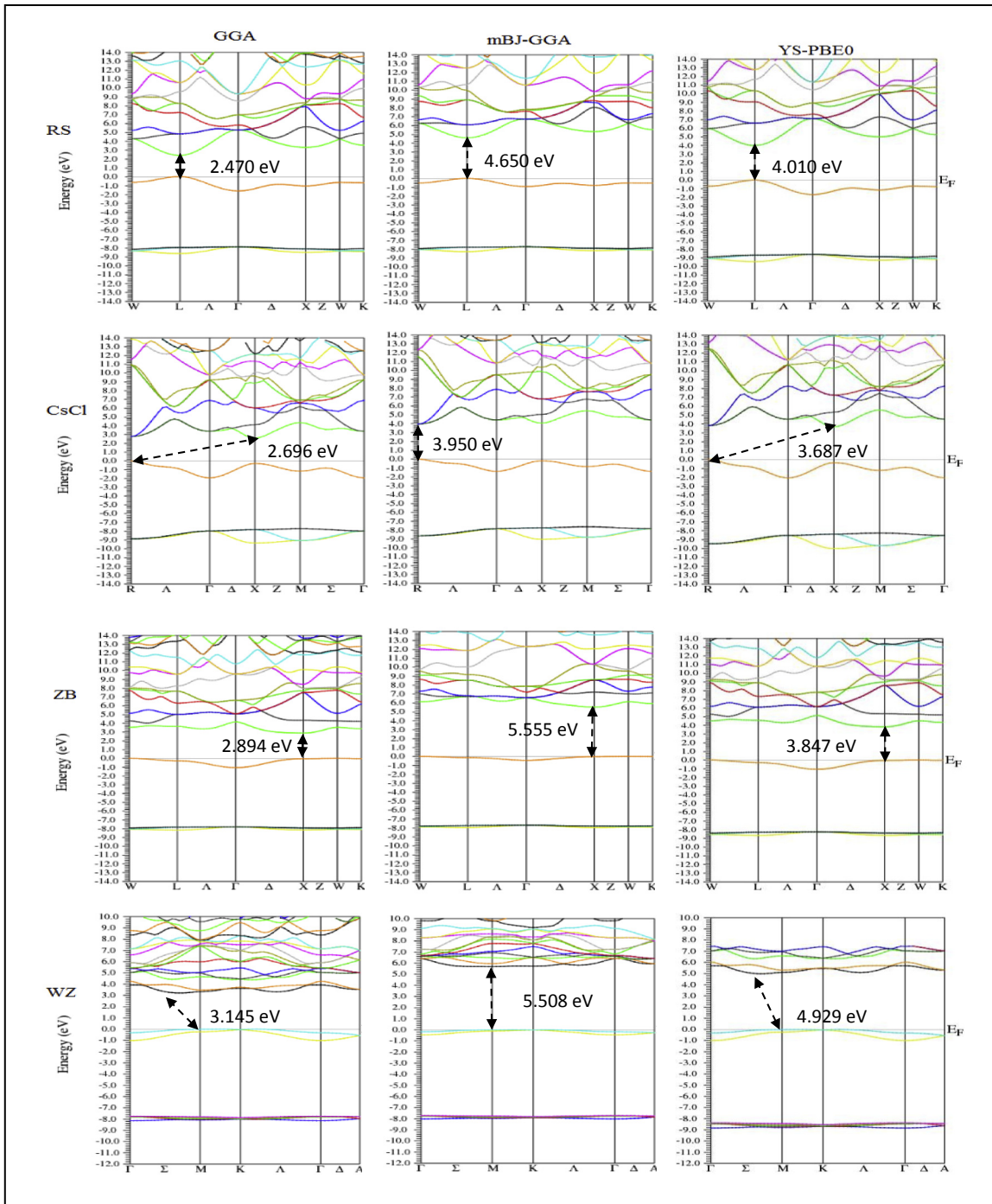


Fig. 9. Band structure of CsH in RS, CsCl, ZB and WZ using the GGA, mBJ-GGA YS-PBE0 approaches.

experimental results with about 0.72eV and 0.25eV for RbH and CsH respectively, while the calculations using YS-PBE0 are greater by about 0.245eV and 0.39eV for RbH and CsH respectively. This mainly due to the using greater temperature and pressure in experiment, theoretical calculations carried out at zero temperature and pressure while experiment carried out at ambient conditions. The energy-band gaps decrease, going from KH to CsH, for the four structures; this result agrees with the experimental [33,34] and theoretical results [5,28,30,31]. The present calculations using

mBJ-GGA and YS-PBE0 are more accurate than the other represented theoretical calculations: there is a difference of approximately 2eV between the experimental results and the results of references 5, 29, 26 and present work using GGA and of approximately 1.6eV between the experimental results and those of Ref. 32. KH and RbH within the CsCl structure seem to be classified as semiconductors when using GGA, while they are classified as insulators when using mBJ-GGA and YS-PBE0 methods. On the other hand, CsH is categorized as a semiconductor in the four structures

Table 7

Calculated energy band-gap values ((Eg(eV)) of KH, RbH and CsH in RS, CsCl, ZB and WZ structures.

Compound	Structure	Present work (E _g)				Other theoretical work (E _g)	Experimental results
		GGA	mBJ-GGA	YS-PBEO α _{opt}	α _{opt}		
KH	RS	L→L 3.428	L→L 6.012	L→L 5.957	0.56	3.5992 ^a , 5.85 ^b , 3.203 ^c , 6.28 ^d	
		R→X 2.456	R→X 4.971	R→X 3.835	0.40	2.0 ^a	
	ZB	W→L 3.671	X→X 6.801	W→L 5.574	0.47		
	WS	M→M 3.655	M→M 6.917	M→M 5.622	0.47		
RbH	RS	L→L 3.050	L→L 5.633	L→L 4.655	0.41	3.0255 ^a , 2.960 ^c , 4.21 ^e 6.97 ^f	4.91 ^h
	CsCl	R→X 2.397	R→X 4.474	R→X 3.830	0.38	2.1 ^a	
	ZB	X→X 3.379	X→X 6.466	X→X 5.171	0.44		
	WS	M→M 3.470	M→Σ 6.907	M→M 5.269	0.44		
CsH	RS	L→L 2.470	L→L 4.650	L→L 4.010	0.41	2.4472 ^a , 4.04 ^e , 6.67 ^f , 2.80 ^g	4.4 ⁱ
	CsCl	R→X 2.696	R→R 3.950	R→X 3.687	0.28	2.5 ^a	
	ZB	X→X 2.894	X→X 5.555	X→X 3.847	0.45		
	WS	M→Σ 3.145	M→M 5.974	M→Σ 4.929	0.45		

^aRef. [5].^bRef. [26].^cRef. [28].^dRef. [29].^eRef [30].^fRef [31].^gRef. [32].^hRef. [33].ⁱRef. [34].

using GGA and an insulator using mBJ-GGA and YS-PBEO approaches. Although the ground state is well described by GGA, this approximation fails to account for excited-state properties. Due to a well-known non-physical problem in calculating the energy-band gap using GGA, which is the self-interaction error [35], differences in energy-band gap values between GGA on one hand and mBJ-GGA and YS-PBEO on the other hand arise. With GGA, the energy-band gap is underestimated, and sometimes a semiconducting or metallic state may be obtained instead of an insulating one.

This problem shifts the alkali-atom states to higher levels, producing increases in the Coulomb repulsion between the alkali-“s” state and H-“s” state; this incorrect interaction lowers the valence-energy band. Becke and Johnson solve this problem by suggesting an exact exchange potential. The topologies of the density of states for the KH, RbH and CsH compounds are quite similar to one another. Fig. 10 displays the densities of states of CsH compounds, obtained using the GGA and mBJ-GGA approaches. The heights of the peaks vary from one structure to another, and depend on the structure and the method used to calculate the exchange potential. By the structural phase transition from the RS to the CsCl structures, the band gaps of these compounds decrease by about 0.7–1.2 eV. Total and partial densities of states for the KH, RbH and CsH compounds with the four structures RS, CsCl, ZB and WZ have been calculated to further understand the nature of electronic-band structures. It is clear that the energy bands below the Fermi energy (FE), indicated by a dotted horizontal line, arise mainly from the H-s states, along with small contributions from X-s and X-p.

Above the FE, they mainly arise from the X-P and X-s states, with a small contribution from the H-s state. Table 7 and Fig. 10 show that the energy-band gap calculated with mBJ-GGA is wider than that calculated with GGA, as mentioned before, and to some extent agree with the experimental results.

4. Conclusions

In the present paper, the structural and electronic properties, in addition to the induced phase-transition pressures of alkali hydrides XH (X = K, Rb and Cs), are calculated in the RS, ZB, CsCl and WZ structures. The FP-LAPW has been used, within the GGA, YS-PBEO and mBJ-GGA approaches, as implemented in the WIEN2k code. Good agreement with the other theoretical and experimental results has been obtained. The energy-band gap was modified by applying the YS-PBEO and mBJ-GGA approaches instead of GGA. YS-PBEO and mBJ-GGA transforms the CsCl structure from semiconductor to insulator for KH and RbH, also semiconductor to wide energy-band gap semiconductor for CsH. By comparing the energy-band gaps for the four structures, we can see that the energy-band gaps decrease as the effective pressures increase. Three phase transitions have been predicted in this work, from RS to CsCl, RS to ZB and RS to WZ, for each compound. It is obvious that XH(X = K, Rb and Cs) undergoes a transition from RS to CsCl under high pressures; the transition pressures are 5.00, 3.50 and 2.54 GPa for KH, RbH and CsH, respectively, with the GGA approach. Under low pressure, the RS structure expands and transforms into WZ and ZB only when V/V₀ is greater than one. It has also been observed that

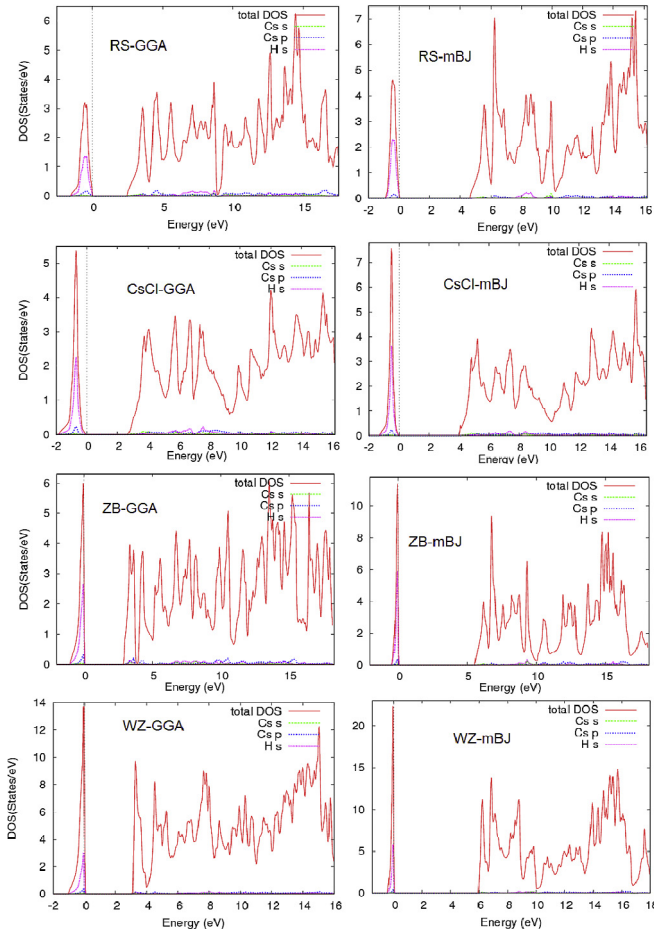


Fig. 10. Density of states of CsH in RS, CsCl, ZB and WZ structures.

the present calculations are in qualitative agreement with the available experimental results and the results of other methods.

Acknowledgments

This work has been carried out in the Computational Physics Laboratory, Physics Department, An-Najah N. University. The authors (Khenata and Bin-Omran) extend their sincere appreciation to the Deanship of Scientific Research at King Saud University for funding this Prolific Research Group (PRG-1437-39). The authors also address their sincere gratitude to Dr. Dibya P. Rai from Pachhunga University-India for the language help.

References

- [1] M.J. Latroche, Structural and thermodynamic properties of metallic hydrides used for energy storage, *Phys. Chem. Solids* 65 (2004) 517.
- [2] K. Ghandehari, H. Luo, A.L. Ruoff, S.S. Trail, F.J. DiSalvo, New high pressure crystal structure and equation of state of cesium hydride, *Phys. Rev. Lett.* 74 (1995) 2264.
- [3] S.J. Duclos, Y.K. Vohra, A.L. Ruoff, S. Filipek, B. Baranowski, High-pressure studies of NaH to 54 GPa, *Phys. Rev. B* 36 (1987) 7664.
- [4] H.D. Hochheimer, K. Strossner, W. Honle, B. Baranowski, F. Filipek, High pressure X-ray investigation of the alkali hydrides NaH, KH, RbH and CsH, *Z. Phys. Chem. NeueFolge* 143 (1985) 139.
- [5] P.G. Sudha, A.T. Asvini, R. Rajeswara, K. Iyakutti, Structural, electronic and elastic properties of alkali hydrides (MH: M = Li, Na, K, Rb, Cs): Ab initio study, *Comput. Mater. Sci.* 84 (2014) 206.
- [6] S. Xiao-We, Q.F. Chen, C. Xiang-Rong, Ab initio study of phase transition and bulk modulus of NaH, *J. Solid State Chem.* 184 (2011) 427.
- [7] A.M. Saitta, D. Alfe, S. de Gironcoli, S. Baroni, Phonon softening and elastic instabilities in the cubic-to-orthorhombic structural transition of CsH, *Phys. Rev. B* 78 (1997) 4958.
- [8] C.O. Rodriguez, M. Methfessel, Pressure-induced phase transformations in alkali-metal hydrides calculated using an improved linear muffin tin orbital atomic sphere approximation energy scheme, *Phys. Rev.* 45 (1992) 90.
- [9] R. Ahuja, O. Eriksson, B. Johansson, Theoretical search for the CrB-type high-pressure phase in LiH, NaH, KH and RbH, *Physica B* 265 (1999) 87.
- [10] R. Jaradat, M. Abu-Jafar, I. Abdelraziq, R. Khenata, D. Varshney, S. Bin-Omran, S. Al-Qaisi, High-pressure structural phase transition and electronic properties of the alkali hydrides compounds XH (X = Li, Na), *Phase Transitions* (2017) 1–14. <https://doi.org/10.1080/01411594.2017.1286488>.
- [11] P. Blaha, K. Schwarz, P. Sorantin, S.B. Trickey, Full-potential linearized augmented plane wave programs for crystalline systems, *Comput. Phys. Commun.* 59 (1990) 399.
- [12] P. Hohenberg, W. Kohn, Inhomogeneous electron gas, *Phys. Rev.* 136 (1964) 864.
- [13] P. Blaha, K. Schwarz, G. Madsen, D. Kvasnika, J. Luitz, WIEN2k, Technical-Universität Wien, Austria, 2001. ISBN 3-9501031-1-2.
- [14] J.P. Perdew, S. Burke, M. Ernzerhof, Generalized gradient approximation made simple, *Phys. Rev. Lett.* 77 (1996) 3865.
- [15] F. Tran, P. Blaha, Accurate band gaps of semiconductors and insulators with a semi local exchange-correlation potential, *Phys. Rev. Lett.* 102 (2009) 226401.
- [16] A. Becke, M. Roussel, Exchange holes in inhomogeneous systems: a coordinate-space model, *Phys. Rev.* 39 (1989) 3761.
- [17] F. Tran, P. Blaha, Implementation of screened hybrid functionals based on the Yukawa potential within the LAPW basis set, *Phys. Rev. B* 83 (2011) 235118.
- [18] H.J. Monkhorst, J.D. Pack, Special points for Brillouin-zone integrations, *Phys. Rev.* 13 (1976) 5188.
- [19] F.D. Murnaghan, The compressibility of media under extreme pressures, *Proc. Natl. Sci. USA* 30 (1944) 244.
- [20] W. Pearson, P. Villars, L.D. Calvere, *Persson's Handbook of Crystallographic Data for Intermetallic Phases*, ASM, Metals Park, Ohio, 1985.
- [21] E. Zintl, A. Harder, UberAlkalihydride, *Z. Phys. Chem. Abt* 14 (1931) 265.
- [22] I.O. Bashkin, T.N. Dymova, E.G. Pomyatovskii, On the structural transition from NaCl to CsCl type in Alkali hydrides, *Phys. Status Solidi* 100 (1980) 87.
- [23] S.E. Gulebaglan, E.K. Dogan, M.N. Secuk, M. Aycibin, B. Erdinc, H. Akkus, First-principles study on electronic, optic, elastic, dynamic and thermodynamic properties of RbH compound, EDP Sciences, *Int. J. Simul. Multisci.Des.Optim* 6 (2015) A6. <http://creativecommons.org/licenses/by/4.0/>.
- [24] G.D. Barrera, D. Colognesi, P.C.H. Mitchell, A.J. Ramirez-Cuesta, LDA or GGA? A combined experimental inelastic neutron scattering and ab initio lattice dynamics study of alkali metal hydrides, *Chem. Phys.* 317 (2005) 119.
- [25] L. Engrebretsen, Electronic Structure Calculations of the Elastic Properties of Alkali Hydrides, Graduation Thesis, Royal Institute of Technology KTH, Stockholm, 1995.
- [26] Z. Jingyun, Z. Lijun, C. Tian, L. Yan, H. Zhi, M. Yanming, Z. Guangtian, Phonon and elastic instabilities in rocksalt Alkali hydrides under pressure: A first-principles study, *Phys. Rev. B* 75 (2007) 104115.
- [27] S. Lebègue, B. Arnaud, M. Alouani, P.E. Blochl, Implementation of an all-electron GW approximation based on the projector augmented wave method without plasmon pole approximation: Application to Si, SiC, AlAs, InAs, NaH, and KH, *Phys. Rev. B* 67 (2003) 155208.
- [28] V.I. Zinenko, A.S. Fedorov, First principle calculations of alkali hydride electronic structures, *Sov. Phys. Solid State* 36 (1994) 742.
- [29] V. Luan, L. Pueyo, Simulation of ionic crystals: the ab initio perturbed-ion method and application to alkali hydrides and halides, *Phys. Rev. B* 41 (1990) 3800.
- [30] N. Novakovic, I. Radisavljevic, D. Colognesi, S. Ostojic, N. Ivanovic, First principle calculations of alkali hydride electronic structures, *J. Phys. Condens. Matter* 19 (2007) 406211.
- [31] R.C. Bowman, Cohesive energies of the alkali hydrides and deuterides, *J. Phys. Chem.* 75 (1971) 1251.
- [32] P. Vajeeston, Theoretical Modeling of Hydrides, PhD thesis, University of Oslo, 2004.
- [33] K. Ghandehari, H. Luo, A.L. Ruoff, S.S. Trail, F.J. DiSalvo, Crystal structure and band gap of rubidium hydride to 120 GPa, *Mod. Phys. Lett.* 9 (1995) 1133.
- [34] K. Ghandehari, H. Luo, A.L. Ruoff, S.S. Trail, F.J. DiSalvo, Band gap and index of refraction of CsH to 251 GPa, *Solid State Commun.* 95 (1995) 385.
- [35] J.P. Perdew, A. Zunger, Self-interaction correction to density-functional approximations for many-electron systems, *Phys. Rev.* 23 (1981) 5048.